

# Germanium/silica ratio and trace element composition of Early Cambrian siliceous rocks in Keping: implications for the siliceous rocks' formation and paleoenvironment interpretations

Zixuan Guan<sup>1</sup> · Shibiao Deng<sup>1</sup> · Peixian Liu<sup>1</sup> · Yiqiu Jin<sup>2</sup> · Xingchun Cao<sup>1</sup>

Received: 8 May 2020 / Revised: 10 August 2020 / Accepted: 16 September 2020 / Published online: 28 September 2020  
© Science Press and Institute of Geochemistry, CAS and Springer-Verlag GmbH Germany, part of Springer Nature 2020

**Abstract** This study used the germanium/silica (Ge/Si) ratios, together with rare earth elements and other trace elements to infer the siliceous source and sedimentary environment of the siliceous rocks located at the bottom of Yuertusi Formation in Northwestern Tarim Basin, Keping, China. Previous studies have shown that this siliceous rock stratum formed at the edge of the carbonate platform on the continental shelf. Researchers suggest that these siliceous rocks were formed by hydrothermal activity, but some still draw different conclusions. Understanding the silicon source and depositional environment of these siliceous rocks would help us learn the processes of environmental changes and the causes of biological explosions during this period. The value of germanium/silica ratios of these siliceous rocks is from 0.15 to 0.37  $\mu\text{mol/mol}$  and much lower than above 10  $\mu\text{mol/mol}$  values in siliceous rocks that are known formed by hydrothermal activity. All samples are rich in HREE, which differ from hydrothermal siliceous rocks that are rich in LREE. Most samples lack hydrothermal related elements. All these features show that the source of these siliceous rocks' siliceous is not hydrothermal fluids. The samples' Ce/Ce\* range from 0.88 to 1, and Th/U ratios range from 0.01 to 0.36. These features suggest these siliceous rocks were formed in an anoxic environment. Considering all the evidence, we conclude that the siliceous rock stratum at the bottom of

the Lower Cambrian Yuertusi Formation in northwest Tarim Basin, Keping, was formed in anoxic seawater at the edge of the carbonate platform on the continental shelf. Its silicon source is seawater instead of hydrothermal fluid.

**Keywords** Siliceous rocks · Trace elements · Ge/Si ratio · Tarim Basin

## 1 Introduction

The Ediacaran–Cambrian transition is a primary node in the evolution of the global paleoenvironment, during which major geology events such as “Snowball Earth,” “Super-continental Cracking,” and “Cambrian Explosion” had occurred. This process is fully recorded in the Yangtze and Tarim platforms in China (Zhang et al. 2016). The Lower Cambrian black rock series (the Black Shales) in the Yangtze platform has important features such as a poly-metallic enrichment layer (Ni–Mo–V–Au) and the Oceanic Anoxic Event (OAE), and have received in-depth studies in geosciences (Li et al. 2015). However, the Early Cambrian Ocean's environmental data in the Tarim Basin is quite scarce compared with the black shale. Research in this area is also lacking.

The Yuertusi Formation in the northwest Tarim basin is formed in the Early Cambrian era. The stratigraphic horizon is equivalent to the Blake Shales in the Yangtze platform. Similar to the Blake Shales, several layers of siliceous rock appear at the bottom of Yuertusi Formation. The siliceous rock is a kind of sediment rock formed in chemical or biochemical processes. Meaningful and abundant geochemical information in siliceous rock can be well persevered for long periods of time because of the dense structure and stable chemical properties of siliceous

✉ Zixuan Guan  
guanzixuan2016@pku.edu.cn

<sup>1</sup> MOE Key Laboratory od Orogenic Belts and Crustal Evolution, School of Earth and Space Science, Peking University, Beijing 100871, China

<sup>2</sup> Research Institute of Petroleum Exploration and Development, CNPC, Beijing 100083, China

rock (Chunlong 2001). Two main sources of siliceous materials can form siliceous rocks. One is from weathering on the continent, and the other is from deep earth (Hesse 1989). About 80% of soluble SiO<sub>2</sub> in seawater is from the continent, and the other 20% is from deep-Earth (Treguer et al. 1995; Froelich et al. 1989). These two kinds of rocks from different siliceous sources have different trace element compositions. Thus, they can be distinguished by analyzing their trace elemental composition.

Many researchers have focused on the sources and the sedimentary environment of this siliceous rock recent years. Several different opinions about the sources of this siliceous rock have been stated. Sun et al. (2008) studied trace elements and rare earth elements of the siliceous rocks in this area, and suggest that siliceous rock is likely deposited from hydrothermal fluid and formed in continental margin-abyssal environment. Bingsong et al. (2004) analyzed trace elements of the siliceous rocks samples taken from Sholbrak section located at east Keping and concluded that the upwelling current carries the substances formed in the pelagic ocean floor onto the shelf to deposit those siliceous rocks. Sun et al. (2008) studied noble gas isotopes from inclusions of the siliceous rock taken from Sholbrak (east of Keping) and Shuiquan (south of Kuruktag). They suggest that the siliceous rocks formed on the continent shelf and its siliceous was from submarine volcano activity and transported to the continental shelf by hydrothermal plumes. Chen et al. (2010) analyzed  $\delta^{30}\text{Si}$  and  $\delta^{18}\text{O}$  of bedded siliceous rocks at the bottom of Cambrian strata and cherts-bearing dolostone on the top of Cambrian strata. They believe that the bedded siliceous rocks are sedimentary sources. Yin et al. (2015) think the siliceous rocks formed in the deep-basin and related to hydrothermal activity by analyzing their main elements and trace elements.

In general, most researchers believe that the siliceous rocks at the bottom of the Yuertusi Formation in the northwestern margin of the Tarim Basin have a certain level of relationship with hydrothermal fluids, and their tectonic location is close to the oceanic basin. However, there are also views that these siliceous rocks are mainly from seawater deposition. Exploring the siliceous source and depositional environment of these siliceous rocks will help us understand the processes of environmental changes and causes of biological explosions during this period.

Previous studies mainly used rare earth elements and trace elements to find the siliceous rock's material source. However, due to the diverse nature of these elements and multiple sources, it is impossible to define the source of siliceous rock firmly. This research uses a decisive method: germanium/silica (Ge/Si) ratio, combined with rare earth elements and trace elements geochemical characteristics, to

study the sedimentary environments and the siliceous source of siliceous rocks in this region.

## 2 Geological settings

The Tarim Basin is located in the northwest of China. Being the largest basin in China, it is about 0.56 million kilo squares. The basin was almost covered by desert. The west rim of the basin is Palmier highland, the north rim is Tianshan Mountains, and the south rim is the west Kunlun Mountains and Arkin Mountains (Zhiqin et al. 2011).

This area of interest is in the northwest margin of Tarim Basin, Wushi County, Arksu (Fig. 1). In this area, the continued strata from Ediacaran to Ordovician is distributed in several nappe belts. The rocks in these strata are mainly carbonate, including limestone and dolomite. The siliceous rocks are at the bottom of the Yuertus Formation, the earliest stratum of the Cambrian.

The Yuertus Formation can be divided into two parts. The upper part of this formation mainly consists of sandy dolomite with a little chert, and the lower part mainly banded siliceous rocks and black shales. The stratum under the Yuertus Formation is Qigebuluk Formation, and there is a parallel unconformity between these two strata. The overlay stratum is Xiaoerbuluk Formation, which is also separated by a parallel unconformity with Yuertus Formation. The sedimentary environment of Yuertus Formation was a margin of carbonate reef located upon the continental shelf. The sedimentary environment was deep-water, and the water depth became shallow gradually over time. But its sedimentary environment was a continental shelf environment overall (Deng 2017).

## 3 Background: Ge/Si ratio

Germanium is one of the Carbon group elements and has similar chemical properties with silicon. Only a few kinds of minerals are rich in Ge, most of Ge in the crust is in the dispersive state. Because of these properties, Ge is like the “isotope” of Si in rocks. Similar to other stable isotope systems, the abundance of Germanium in geological samples is always expressed in the Ge/Si ratio, which is the ratio of the amount of substance of these two elements in samples. Because of the sizeable abundant difference between Ge and Si, the unit of the Ge/Si ratio is  $\mu\text{mol/mol}$ .

According to the study made by Froelich et al., Germanium is more likely to come into clay minerals instead of transported in a dissolved state, so the Ge/Si ratio in river water is low (Froelich et al. 1992). This effect is related to weathering strength. The more substantial weathering leads to a lower Ge/Si ratio in river water. The

average value of the Ge/Si ratio of global rivers water is about 0.54  $\mu\text{mol/mol}$  (Froelich et al. 1992; Mortlock and Frohlich 1987). The Ge/Si ratio of hydrothermal fluid is much higher than groundwater, so the siliceous rocks formed by hydrothermal activity also have a high Ge/Si ratio ranging from 8 to 13  $\mu\text{mol/mol}$  (Mortlock et al. 1993). The Ge/Si ratio of seawater is affected by both river water from continents and hydrothermal fluid from mid-ocean ridges. Modern seawater's Ge/Si ratio is about 0.72  $\mu\text{mol/mol}$  and much lower than hydrothermal fluid. So, Ge/Si ratio is a useful tool to identify the primary sources of siliceous rocks.

The method mentioned above has been used to find out the siliceous source of silica part in BIF. Researchers measured the samples taken from BIFs in Precambrian Hamersley formation in west Australia. It shows that the bands rich in iron have a higher Ge/Si ratio than the poor silica bands and have ten times the difference. The result suggested that the iron and silica in BIFs may have different sources (Hamade et al. 2003). Dong et al. had

researched the cherts in Laopu formation at the Silikou section, Guangxi province. They find the siliceous component in the samples had low Ge/Si ratios range from 0.4 to 0.6  $\mu\text{mol/mol}$ , and suggest that the siliceous source of the chert should be seawater instead of hydrothermal fluid (Dong et al. 2015; Cui et al. 2019).

## 4 Sampling and analytical procedures

### 4.1 The sections and the samples

This study took 17 samples from 3 sections in the study area. Most of the samples were taken from the Jinlinkuang section which had the thickest siliceous rock layer in three sections, and these samples' name starts with "JLK". The other two sections were the Sugate-Bulak section and Kulunan section. The location of these three sections was marked in Fig. 1. The followings are the detail of these three sections and the samples taken from them.

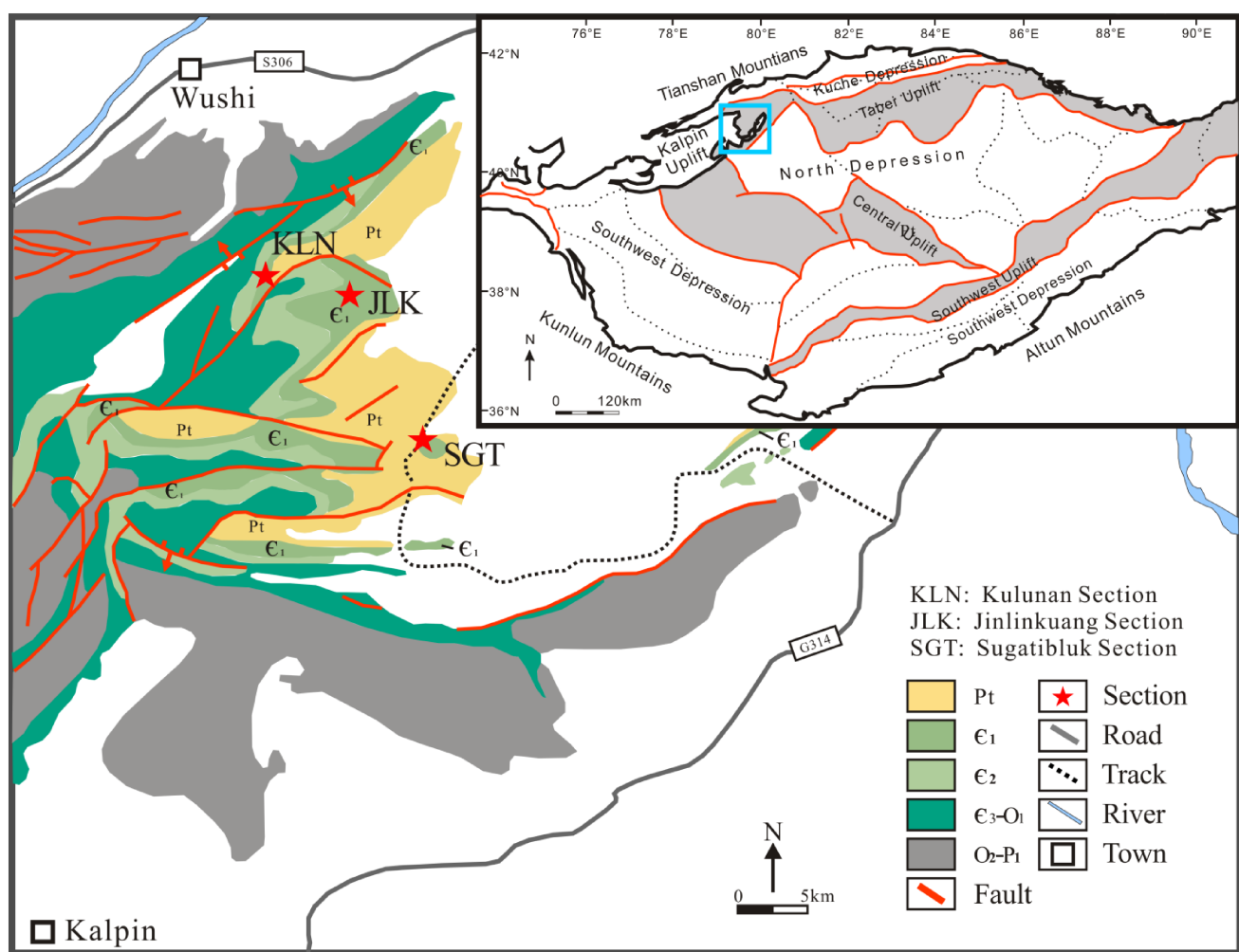
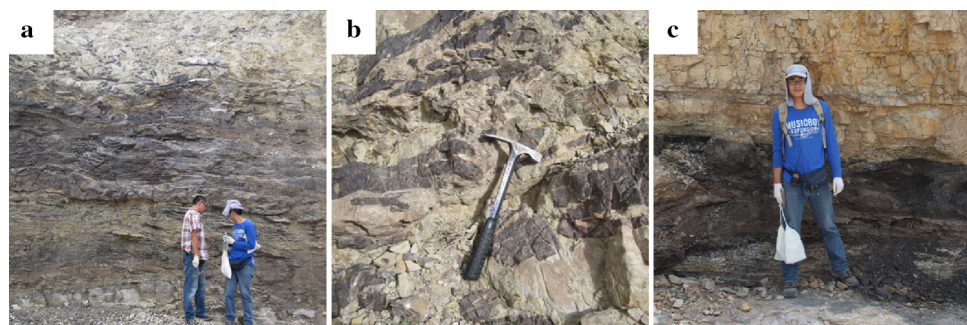


**Fig. 1** Brief structure setting of Tarim Basin and location of the research zone. (Modified from Jia 1997; Deng 2017)

**Fig. 2** Field photographs of siliceous rocks in the Yuertus formation from three sections.  
**a** Jinlinkuang section (JLK),  
**b** Kulunan section (KLN),  
**c** Sugate-Bulak section (SGT)



Jinlinkuang section (JLK) lay in the center of the research zone. Its coordinate is  $41^{\circ}2'40.44''$  N,  $79^{\circ}25'7.16''$  E. The thickness of the Yuertus Formation in this section is 15 m and can be divided into six layers (Fig. 2).

From bottom to top, the first layer is a thin layer siliceous rock, and the thickness is 0.3 m. The second is the thin layer siliceous rock interlayer with thin layer phosphorus mudstone, and the is 2.5 m thick. The third is a thin layer of siliceous rock, and its thickness is 1.5 m. The fourth layer is about 1 m thick and is a siliceous rock interlayer with dolo-mudstone. The fifth layer is sand dolomite with some siliceous bands, and these bands are cluttered. This layer is about 3 m thick. The top layer of this formation in this section is sand-dolomite and has no siliceous rock in it.

The Kunlunan section (KLN) lay in the northwest of the research zone and near the Jinlinkuang section. Its coordinate is  $41^{\circ}3'41.79''$  N,  $79^{\circ}17'53.95''$  E. The total thickness of the Yuertus Formation in this section is 19 m and can be divided into four layers. The siliceous rocks can be seen at the lower two layers in this section. The first layer is a thin layer of siliceous rock, and its thickness is 4 m. The second layer is a siliceous rock interlayer with dolomite, and it is 4.5 m thick. The third and the fourth layer is mainly consisting of sand-dolomite, almost no siliceous in it.

Sugate-Bulak section (SGT) lay in the south of the research zone. Its coordinate is  $40^{\circ}54'22.84''$  N,  $79^{\circ}28'45.70''$  E. The total thickness of the Yuertus Formation in this section is 22 m and can be divided into four layers. The siliceous rocks only appeared at the lower two layers in this section. The first layer is a thin layer siliceous rock interlayer with thin black shale with about 1 m thick. The second layer is light yellow dolomite with some chert nodules in it and is 2 m thick.

The siliceous rocks can be divided into two types of layered siliceous rock and banded siliceous rock with chert nodule in dolomite. The two types of siliceous rocks can be found in all of those sections mentioned above. The rock columns and sampling locations of these sections can be seen in Fig. 3.

## 4.2 Microscopy

The slice observation found that all samples' siliceous parts are made by chalcedony. The layered type and non-layered type have no significant difference in micromorphology. The chalcedony in siliceous rocks is granular, and the size of grains ranges from 5 to 10  $\mu\text{m}$ , some chalcedony grains have a flower-like shape and twisted contact with others. The chalcedony is colorless and clear in the monoscopic observation. Its interference color is grey or light blue under the orthoscope. Some grains are yellow or brown color because of the impurities (Fig. 4a). There are many lumps in most of these samples. Most of the lumps are brown or black and opaque. The shape of most lumps is an irregular bar. Their long axis length ranges from 100 to 500  $\mu\text{m}$ , and the short-axis ranges from 50 to 200  $\mu\text{m}$  (Fig. 4b). There are many small ferric particles distributed in chalcedony. The size of the ferric particles ranges from 1 to 5  $\mu\text{m}$  (Fig. 4c). No large barite crystal has been found in all slices, the barite may be small particles or hide in opaque lumps. Some fossils are recognized in several slices, most of them are Cyanobacteria, sponge, or Algae. Well-preserved fossils: *Megathrix longus*, has been found in JLK-02 (Fig. 4d).

## 4.3 Analysis steps

### 4.3.1 Pretreatment

Siliceous parts were hand-picked from samples and were crushed to 200 meshes by using an electromagnetic grinder. The powder sample was repeatedly washed in 1 N HCl for three times to remove calcareous content. The calcareous-free insoluble residue was then subjected to 3 additional washes by deionized water and dried down in a Drying Cabinet at 65 °C.

About 100 mg carbonate-free sample was dissolved in a Teflon beaker by a mixture of 3 mL concentrated HF and 1 mL concentrated  $\text{HNO}_3$  at 120 °C for 48 h. The solution was dried down in a hotplate, and the residue was then dissolved in 3 mL concentrated  $\text{HNO}_3$  at 120 °C for 24 h.

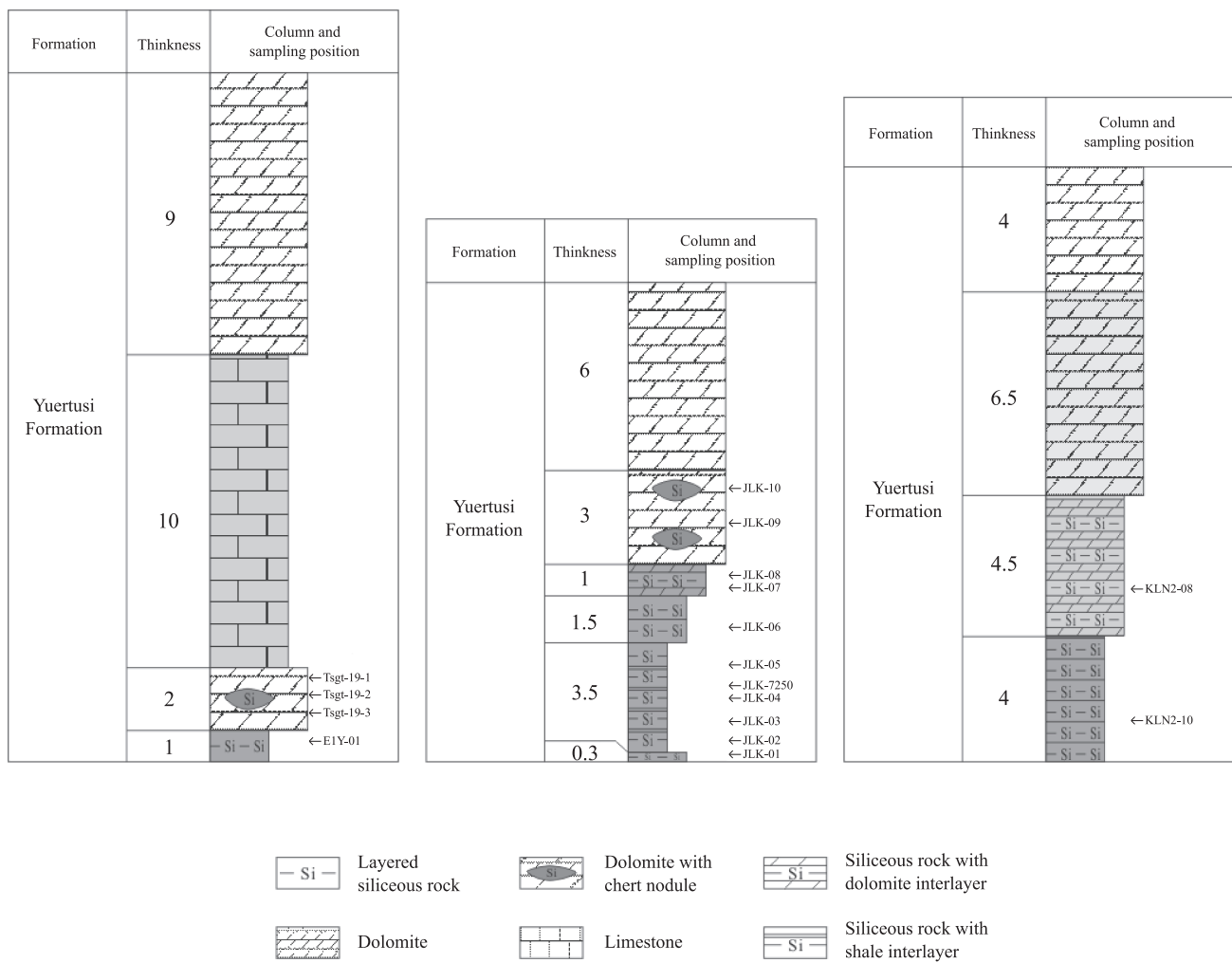


**Fig. 3** The strata columns of three sections and the sampling location

After dried down in a hotplate, the residue was then dissolved in 2% HNO<sub>3</sub> for elemental composition analyses. This dissolution procedure would cause silica loss due to the formation of volatile SiF<sub>4</sub>, while Ge would be retained in solution because of the high boiling point of GeF<sub>4</sub> at 300 °C.

#### 4.3.2 ICP-OES and ICP-MS

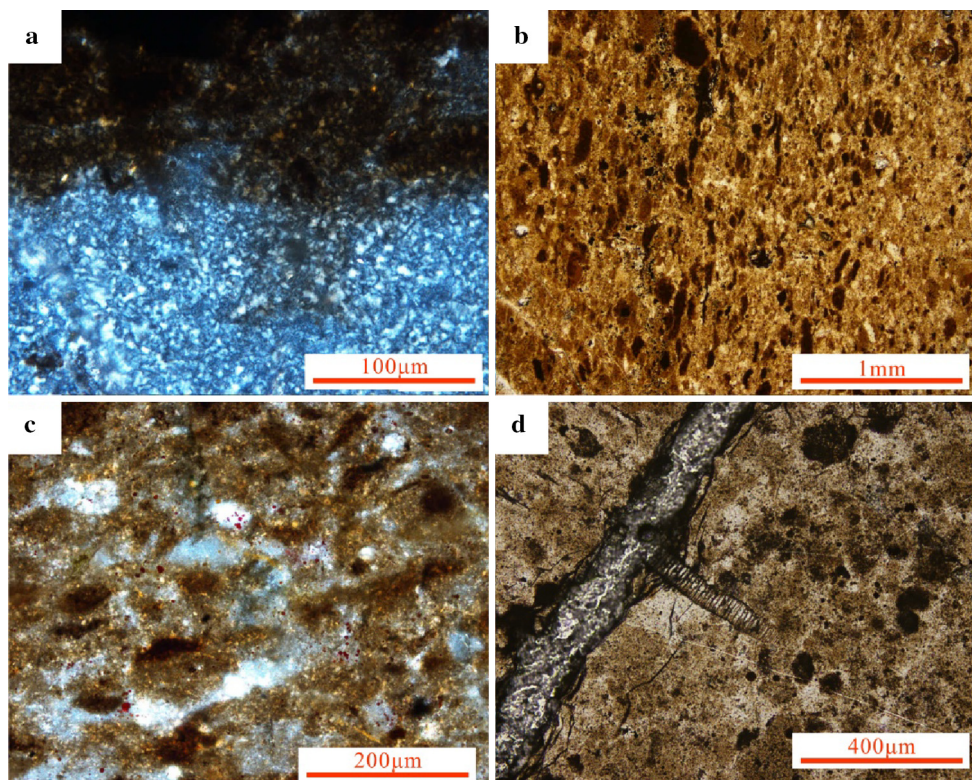
The major elemental compositions were determined by an inductively-coupled-plasma optical emission spectrometer (ICP-OES) at Peking University. At the same time, the trace element contents were measured by an ICP mass spectrometry (ICP-MS) at the Chinese Academy of Geological Sciences. The elemental compositions were calculated on the carbonate-free basis, and all major and minor elements are considered as oxides (i.e., Na<sub>2</sub>O, MgO, Al<sub>2</sub>O<sub>3</sub>, SiO<sub>2</sub>, K<sub>2</sub>O, CaO, FeO, MnO, P<sub>2</sub>O<sub>5</sub>, TiO<sub>2</sub>). The silica content was determined by the bulk sample weight

(carbonate-free) minus the total weight of all other oxides. The analytical precisions are better than 10% for both ICP-OES and ICP-MS analyses.

#### 4.3.3 Interference from BaO polyatomic ions

The Ba element in the sample will interfere with the Eu measurement when using ICP-MS to measure rock samples. Some polyatomic ions of Ba may have similar masses to Eu (Bi et al. 2016; Guan et al. 2013). Similar phenomena have also been observed in our data. There are linear correlations between the measured values of Ba and Eu and the measured values of Ba and Sm (Fig. 5). There are methods for correcting measurement data using standard samples or mathematical methods. However, in our research, the Ba content of the sample is too high, and the laboratory's conventional correction methods are not very effective.

**Fig. 4** Photomicrographs showing the texture of siliceous rocks of Yurtus formation. **a** JLK-07. Chalcedony under crossed polars. Some of the impurities show yellow or brown; **b** JLK-03. Lumps with black color; **c** JLK-07. Small ferric particles distributed in chalcedony; **d** JLK-02. Fossils in rocks, especially *Megathrix longus*



## 5 Results and discussions

### 5.1 Ge/Si ratio

The elemental compositions and Ge/Si ratios are listed in Table 1. All samples have high SiO<sub>2</sub> and a low Ge/Si ratio. The samples' Ge/Si ratios range from 0.15 to 0.37 (n = 17, average = 0.249), the average values of layered and non-layered siliceous rocks are 0.227 (n = 9) and 0.277 (n = 8). There is no significant difference between the two types, and they are both much lower than the siliceous rock form by hydrothermal activity. That is, the result of the Ge/Si ratio shows that the siliceous source of siliceous rocks at the bottom of Yuertus formation is seawater.

### 5.2 Major element contents

17 siliceous rock samples' major element compositions were analyzed and listed in Table 1. All samples have high Si content, while other major element contents are lower than 5%. All samples have extremely low Mn content (1–10 ppm).

Al and Ti come from continent weathering, while Fe and Mn are from hydrothermal fluids (Murray et al. 1990, 1991; Murray 1994). Bostrom thought the elements Al, Fe, and Mn can be used to distinguished the sources of sediment and sedimentary rock, and made a Fe–Al–Mn tri-

graphic and Al/(Al + Fe + Mn) index (Boström and Peterson 1969). Adachi then used this index and graphic in siliceous rocks study (Adachi et al. 1986).

In this study, the content of Al is higher than Fe in most samples except JLK-01. Most samples have high Al/(Al + Fe + Mn) range from 0.80 to 0.95 (n = 16, average = 0.907), but JLK-01 is 0.224. The average value of layered siliceous rock samples and non-layered siliceous rock samples is 0.823 (n = 9, include JLK-01) and 0.916 (n = 8). Both two types of siliceous rock are rich in Al. The major elements suggested that most of the siliceous rocks came from seawater instead of hydrothermal fluid.

### 5.3 REE feature of siliceous rocks

We analyzed the rare earth element composition of 17 samples, which are listed in Table 2. The data in this table for Sm, Eu, and Gd are corrected values. The total REE of these samples is 1.33 to 4.72 ppm, the total REE of layered siliceous rocks is 1.92 to 4.72 ppm (average = 3.53 ppm, n = 9), and the total REE of non-layered siliceous rocks is 1.33 To 4.07 ppm (average value = 2.31 ppm, n = 8).

#### 5.3.1 REE patterns

The REE data was normalized against PAAS (McLennan 1989) and plotted in Fig. 6. All samples have similar REE

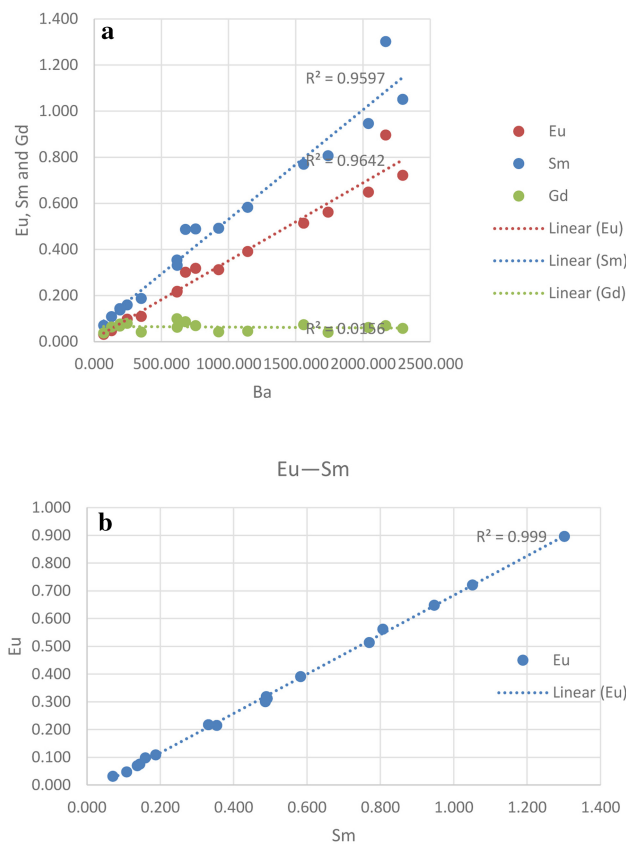


**Fig. 5** **a** The chart of correlation between Ba and Eu, Sm, Gd. Eu and Sm are greatly affected by Ba content, while Gd is not significantly affected. **b** The chart of the correlation between Eu and Sm. Eu and Sm have a linear correlation

patterns. They are rich in HREE. The La/Yb values of all samples are range from 0.59 to 2.53, the layered siliceous rocks' La/Yb values are from 0.61 to 2.53 (mean = 1.04, n = 9), the non-layered siliceous rocks' La/Yb values are from 0.59 to 1.72 (mean = 0.92, n = 8).

These features are similar to dolomites' REE features from Ordovician Sholbrak formation in the same area (Zhang et al. 2014). These dolomites are formed by early burial dolomitization instead of hydrothermal fluid. These samples are all enriched with HREE, which is one of the important features of seawater. It is also an obvious difference in hydrothermal fluid (Douville et al. 1999; Zhenju et al. 2000). This is one of the pieces of evidence that the siliceous source of these siliceous rocks is seawater.

### 5.3.2 Ce anomaly

Ce is an element sensitive to the changing of the redox environment. The seawater in the oxidizing conditions always shows obviously low Ce/Ce\* value, while a Ce/Ce\* value nearly 1 or higher than 1 means reducing habitat (German et al. 1991). Ce anomaly values were calculated

by  $\text{Ce}/\text{Ce}^* = \text{Ce}_N / \sqrt{\text{La}_N \times \text{Pr}_N}$ , the subscript N means the normalized values of elements. The Ce/Ce\* of samples were shown in Table 2. Samples' Ce/Ce\* values range from 0.51 to 0.90, and the average is 0.628. The layered siliceous rock samples' Ce/Ce\* values are range from 0.52 to 0.63 (mean = 0.572, n = 9) and the non-layered siliceous rock samples' values are range from 0.51 to 0.90 (mean = 0.684, n = 8). No significant difference between the two kinds of siliceous rock on Ce/Ce\* value. Besides, according to Murray's studies, the siliceous rocks formed in mid-ocean ridge, deep-sea basin, and continent margin have significant differences in Ce/Ce\* value. The typical value of these three kinds is 0.29, 0.55, and 1.30 (Murray et al. 1990, 1991; Murray 1994). The samples' Ce/Ce\* values in this study are in the middle of the last two types. The slightly negative Ce anomalies suggest two kinds of siliceous rock were both formed in an anoxic environment.

## 5.4 Other trace elements features

### 5.4.1 U and Th/U ratio

At the surface environment, the element Th shows in valence + 4 and always forms insoluble compounds. The U shows valence + 4 in an anoxic environment and forms insoluble compounds. However, in the oxidizing conditions, the U shows valence + 6 and forms soluble compounds in water. Therefore, the U element can transport by water in an oxidizing condition but will settle down in an anoxic environment. The average content of the Th element is a little higher than the U element in the crust. According to this law, if the Th/U ratio is lower than 1.0 and U element content is higher than Th element in sedimentary rock, this rock may form in an anoxic environment (Huajin et al. 2009). This method had been used in much sedimentary research for finding out the redox status of sedimentary environments (Sun et al. 2008; Bingsong et al. 2004; Yin et al. 2015; Liu and Zheng 1993).

The data of U, Th element, and Th/U ratio was listed in Table 3. JLK-07 has an extremely high U content. This sample may be contaminated and not counted. All samples in this study had high U values. The Th/U values of layered siliceous rock samples range from 0.02 to 0.13 (mean = 0.07, n = 9), the Th/U value of non-layered siliceous rock samples are range from 0.03 to 0.22 (JLK-07 was not included, mean = 0.14, n = 7). This result shows that these siliceous rocks formed in an anoxic environment. This result is consistent with the Ce/Ce\*'s result on the redox environment.

**Table 1** Major element compositions and Ge/Si of samples

Sample	Section	Weight (mg)	Na <sub>2</sub> O (%)	MgO (%)	Al <sub>2</sub> O <sub>3</sub> (%)	P2O <sub>5</sub> (%)	K <sub>2</sub> O (%)	CaO (%)	TiO <sub>2</sub> (%)	FeO (%)	SiO (%)	Al/(Fe + Mn + Al)	Ge (ppm)	Ge/Si (μmol/mol)
KLN2-10	KLN	92.800	0.026	0.036	0.622	0.013	0.106	0.048	0.018	0.053	99.079	0.922	0.250	0.209
JLK-01	JLK	96.700	0.020	0.039	0.598	0.114	0.083	0.065	0.014	0.075	96.992	0.224	0.189	0.161
JLK-02	JLK	99.800	0.022	0.033	0.573	0.009	0.094	0.036	0.019	0.092	99.123	0.862	0.207	0.173
JLK-03	JLK	97.200	0.020	0.055	0.733	0.007	0.139	0.046	0.024	0.065	98.910	0.918	0.229	0.191
JLK-04	JLK	91.400	0.033	0.223	1.853	0.004	0.392	0.023	0.064	0.135	97.273	0.932	0.330	0.281
JLK-7250	JLK	93.800	0.025	0.041	0.727	0.002	0.115	0.020	0.022	0.072	98.975	0.910	0.188	0.157
JLK-05	JLK	95.900	0.024	0.084	1.912	0.013	0.209	0.044	0.040	0.131	97.543	0.936	0.372	0.316
JLK-06	JLK	91.700	0.022	0.087	0.963	0.008	0.201	0.020	0.040	0.139	98.519	0.874	0.435	0.366
EY-01	SGT	92.400	0.019	0.031	0.551	0.003	0.081	0.037	0.016	0.111	99.150	0.833	0.222	0.185
Average														
KLN2-08	KLN	92.600	0.022	0.029	0.527	0.007	0.083	0.038	0.029	0.319	98.396	0.823	0.269	0.227
JLK-07	JLK	94.000	0.023	0.038	0.757	0.002	0.143	0.087	0.025	0.059	98.868	0.928	0.241	0.202
JLK-08	JLK	96.000	0.024	0.049	0.701	0.002	0.135	0.051	0.026	0.091	98.921	0.885	0.256	0.214
JLK-09	JLK	98.700	0.018	0.029	0.518	0.004	0.076	0.072	0.016	0.125	99.142	0.805	0.173	0.145
JLK-10	JLK	99.000	0.025	0.053	0.996	0.007	0.153	0.044	0.025	0.057	98.641	0.946	0.403	0.338
Tsgt-19-1	SGT	97.500	0.042	0.092	0.922	0.020	0.174	0.077	0.029	0.059	98.585	0.940	0.412	0.346
Tsgt-19-2	SGT	101.600	0.024	0.073	0.885	0.001	0.157	0.047	0.028	0.046	98.740	0.951	0.391	0.328
Tsgt-19-3	SGT	97.000	0.027	0.080	0.976	0.001	0.171	0.052	0.028	0.055	98.610	0.947	0.423	0.355
Average														

**Table 2** Rare earth element data of siliceous rocks in Yuertusi Formation (unit: ppm)

Sample Id	La 139 (ug/ g)	Ce 140 (ug/ g)	Pr 141 (ug/ g)	Nd 142 (ug/g)	Sm 152 (ug/g)	Eu 153 (ug/ g)	Gd 158 (ug/g)	Tb 159 (ug/ g)	Dy 164 (ug/g)	Ho 165 (ug/g)	Er 166 (ug/ g)	Tm 169 (ug/g)	Yb 174 (ug/g)	Lu 175 (ug/ g)	$\Sigma$ REE	La/ Yb
KLN2-10	0.846	0.622	0.087	0.317	0.058	0.014	0.071	0.009	0.057	0.015	0.048	0.010	0.077	0.012	2.242	0.816
JLK-01	2.422	1.267	0.129	0.362	0.068	0.015	0.069	0.011	0.062	0.014	0.049	0.009	0.071	0.011	4.558	2.529
JLK-02	1.198	0.991	0.109	0.310	0.057	0.012	0.056	0.009	0.050	0.011	0.044	0.010	0.099	0.015	2.970	0.897
JLK-03	1.943	1.511	0.207	0.567	0.066	0.012	0.049	0.006	0.028	0.009	0.039	0.009	0.082	0.012	4.540	1.754
JLK-04	1.777	1.370	0.152	0.390	0.063	0.011	0.043	0.009	0.067	0.023	0.103	0.024	0.211	0.033	4.277	0.621
JLK-7250	0.673	0.583	0.077	0.266	0.049	0.010	0.049	0.008	0.046	0.011	0.046	0.011	0.081	0.013	1.923	0.612
JLK-05	1.734	1.492	0.207	0.636	0.099	0.019	0.080	0.013	0.092	0.024	0.103	0.019	0.179	0.026	4.722	0.715
JLK-06	1.973	1.393	0.150	0.430	0.064	0.013	0.054	0.008	0.055	0.013	0.051	0.010	0.100	0.016	4.330	1.460
E1Y-01	0.961	0.676	0.085	0.250	0.036	0.007	0.031	0.004	0.028	0.007	0.030	0.007	0.063	0.011	2.195	1.122
Average	1.503	1.100	0.134	0.392	0.062	0.013	0.056	0.008	0.054	0.014	0.057	0.012	0.107	0.017	3.529	1.170
KLN2-08	0.572	0.428	0.067	0.232	0.049	0.011	0.057	0.008	0.056	0.013	0.052	0.008	0.071	0.013	1.638	0.592
JLK-07	0.843	0.914	0.118	0.372	0.059	0.012	0.055	0.008	0.067	0.015	0.053	0.011	0.077	0.010	2.613	0.810
JLK-08	0.813	0.838	0.111	0.358	0.057	0.012	0.052	0.008	0.057	0.015	0.058	0.012	0.096	0.014	2.501	0.627
JLK-09	1.285	1.044	0.170	0.484	0.059	0.009	0.028	0.005	0.024	0.007	0.029	0.007	0.055	0.010	3.216	1.718
JLK-10	1.453	1.336	0.202	0.698	0.092	0.016	0.058	0.010	0.054	0.013	0.052	0.008	0.069	0.011	4.071	1.552
Tsgt-19-1	0.446	0.657	0.070	0.260	0.050	0.009	0.037	0.008	0.045	0.011	0.041	0.007	0.047	0.007	1.695	0.698
Tsgt-19-2	0.364	0.524	0.050	0.182	0.034	0.007	0.031	0.005	0.041	0.009	0.034	0.004	0.035	0.007	1.326	0.772
Tsgt-19-3	0.397	0.530	0.057	0.188	0.043	0.008	0.036	0.008	0.035	0.009	0.033	0.006	0.044	0.005	1.399	0.666
Average	0.772	0.784	0.105	0.347	0.055	0.011	0.044	0.008	0.047	0.012	0.044	0.008	0.062	0.010	2.307	0.922

#### 5.4.2 Hydrothermal related elements

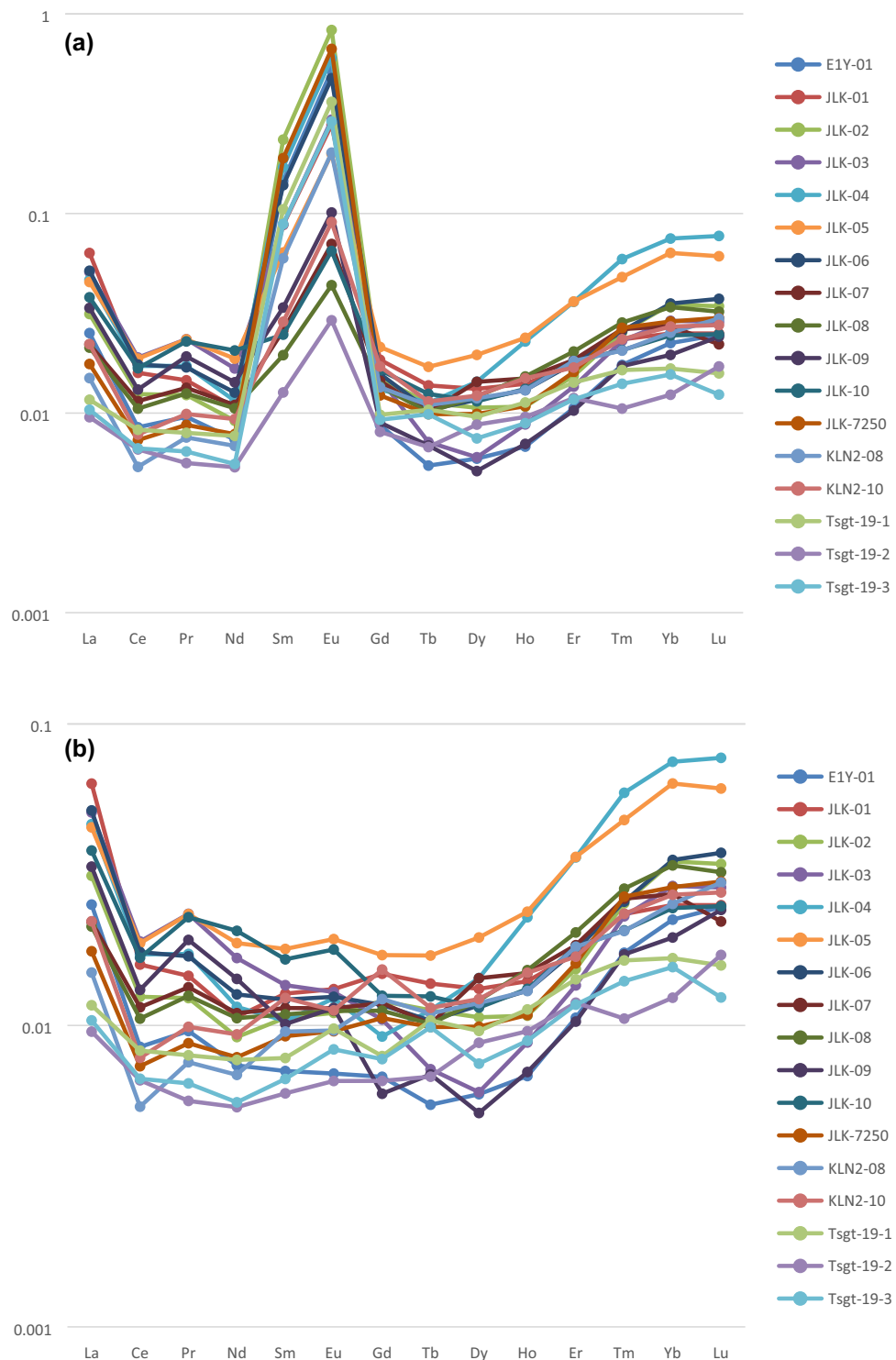
Some elements were always seen as having a strong relationship with hydrothermal activities, such as Ba, As, Sb, Hg, Pb, and Se (Liu and Zhang 1993; Zhou et al. 2000). However, some elements' contents are related to hydrothermal activities, and the redox environment can also be one of the key factors.

Some samples in this study have high Ba contents, but that is not substantial evidence for hydrothermal activities. The layered barite rocks had been founded in many Late Proterozoic and Early Paleozoic strata. These barite rocks were not formed by hydrothermal activity but related to high surface productivity or significant continent weathering (Jewell 2000). According to the research about modern seawater, there are many micrometer-sized barite grains in seawater (Dehairs et al. 1980). These barite grains will deposit on the seafloor with other sediments. The high Ba

contents in sedimentary rocks cannot conclude hydrothermal activities. In this study, no large barite crystal have been founded in samples during the slice observation. If barite is directly crystallized in hydrothermal activity, they would form bigger crystals with size 40–70  $\mu\text{m}$  due to crystal habit than those formed in seawater and this kind of barite can be seen easily in rock slices.

Arsenic (As) is also one of the hydrothermal related elements. However, there is also an element sensitivity to the redox environment because it has a similar nature to sulfur (S). The samples of this study all have higher As values compare with the average value of upper-crust rocks, which is about 1.5 ppm (Taylor and McLennan 1985). The Arsenic contents of layered siliceous rock samples range from 2.16 to 20.90 ppm (mean = 4.56 ppm,  $n = 9$ ), and the non-layered siliceous rock samples' As contents range from 0.96 to 4.32 ppm (mean = 2.23 ppm,

**Fig. 6** **a** The uncorrected REE distribution pattern of siliceous rocks in Yuertusi Formation, data of PAAS come from McLennan (1989). Affected by the excessively high Ba content in the sample, the values of Sm, Eu, and Gd are significantly higher than normal. **b** The REE distribution pattern of siliceous rocks in Yuertusi Formation. Assuming that Sm is not abnormal, the measured values of Sm and Ba are used to correct Eu, and the values of Pr and Ce is used to correct Gd



$n = 8$ ). It seems that this result suggested the As in these siliceous rocks may not come from the continent. However, such low values compared to typical hydrothermal siliceous rocks' As content, which is about 200 ppm (Liu and Zheng 1993), cannot be the evidence of hydrothermal activity.

#### 5.4.3 Trend of elements content on one section

This study had continuously sampled the Jinlinkuang (JLK) section, and 11 samples were obtained. Although different kinds of elements have a significant difference in content, they do have some similarities in their content change

**Table 3** Trace element data of siliceous rocks in Yuerusti Formation (unit: ppm)

Sample	Section	Li	Ti	V	Cr	Co	Ni	Cu	Zn	As	Rb	Mo	Cd	Sn	Sb	Cs	Pb	Th	U	Th/U
KLN2-10	KLN	2.003	112.934	46.233	23.948	0.105	0.892	1.049	5.412	1.364	2.640	0.238	0.013	0.152	0.115	0.181	0.807	0.118	1.484	0.079
JLK-01	JLK	2.727	106.375	342.519	48.155	0.402	28.112	41.181	138.345	20.899	2.732	18.526	0.428	0.128	1.705	0.187	13.331	0.077	4.229	0.018
JLK-02	JLK	2.498	145.237	201.578	101.375	0.127	2.661	5.761	9.141	2.809	3.092	1.506	0.032	0.129	0.558	0.237	1.356	0.173	2.046	0.085
JLK-03	JLK	4.029	177.264	385.007	223.333	0.125	2.972	6.758	12.770	2.287	4.474	0.529	0.018	0.138	0.308	0.313	0.677	0.132	1.654	0.080
JLK-04	JLK	9.529	399.599	1012.571	665.547	0.180	1.888	3.152	15.333	2.293	11.499	0.275	0.028	0.313	0.312	0.844	1.315	0.176	2.593	0.068
JLK-7250	JLK	2.887	132.815	194.814	126.479	0.128	1.459	3.794	9.548	2.161	3.109	0.367	0.018	0.132	0.257	0.277	1.776	0.172	1.293	0.133
JLK-05	JLK	8.325	253.290	442.891	177.835	0.130	1.626	4.285	12.320	3.775	5.689	0.495	0.025	0.216	0.273	0.404	1.328	0.162	2.358	0.069
JLK-06	JLK	4.852	241.354	529.929	150.935	0.254	1.675	1.408	11.266	3.086	5.787	0.395	0.028	0.204	0.257	0.337	1.022	0.102	1.533	0.067
E1Y-01	SGT	1.859	100.233	128.616	83.578	0.138	3.445	2.246	19.105	2.358	2.139	0.498	0.046	0.116	0.454	0.142	1.762	0.098	5.180	0.019
Average	KLN2-08	4.301	185.456	364.907	177.910	0.177	4.970	7.737	25.916	4.559	4.574	2.537	0.071	0.170	0.471	0.325	2.597	0.134	2.486	0.069
Tsgt-19-1	KLN	2.224	107.761	33.936	47.838	0.076	0.590	1.254	2.715	1.302	2.153	0.140	0.004	0.147	0.129	0.152	0.325	0.104	0.918	0.114
Tsgt-19-2	JLK	3.761	164.392	142.571	44.125	0.056	1.641	3.247	5.969	2.883	3.680	0.773	0.016	0.154	0.214	0.234	0.747	0.176	17.085	
Tsgt-19-3	SGT	5.048	190.405	13.446	10.541	0.070	0.598	0.506	6.267	1.531	4.974	0.267	0.013	0.143	0.112	0.288	0.610	0.306	1.523	0.201
Average		3.915	159.146	92.933	42.219	0.074	1.035	2.446	6.328	2.234	3.791	0.397	0.009	0.154	0.140	0.231	0.904	0.197	1.515	0.136

along the section. Figure 7 shows the elements content changing along the section. The trend of elements content has these features:

1. There are two peaks along the section, one is at JLK-01, and the other is at JLK-04. The trace elements can be divided into two groups based on where the peak appears.
2. Cu, As, Mo, Cd, and other several elements peaks at JLK-01 (Fig. 7a). These elements have a common feature: they all belong to siderophile elements or chalcophile elements. These elements often enrich in reducing conditions. The major elements, Fe and P, also peak at the same position. These elements also have high value in deep basin sediment.
3. Li, Ti, V, Cr, and other several elements peak in JLK-04(Fig. 7b). Most of these elements are belong to lithophile elements and always considered to be the elements representing continental sources. The major elements, Al and K, also peaks in the same position.
4. These two groups do not have an intersection. Some elements which peak in JLK-04 even have the lowest value in JLK-01.

Based on these features, we believe a little shale may pollute the sample JLK-04. It can also be evidence of a significant terrestrial input event; JLK-01 may form in a strong reducing, even euxinic environment.

However, according to previous studies about the sedimentary environment and paleogeography in this region, there should be a continental shelf margin environment. One explanation is that upwelling water brought the deep basin water to the shelf, which is also the view of Yu et al. (2004).

## 6 Contrast with other studies

Different research about the siliceous rocks in this district had been done in the last 20 years. However, most of these researches were forces on the east part of this district near Arcsu instead of the area in which these three sections were located.

In this study, the average value of samples' Fe and Mn content is lower than the study made by Yin et al. (2015). The Ce/Ce\* values in this study are about 0.88–1 and higher than Yu's result (Bingsong et al. 2004). The average contents of trace elements such as As in this study are lower than Sun's result (Sun et al. 2008). The difference in analytical procedures and measurement methods may lead to the difference in data. However, these differences between this study and other studies suggest that these siliceous rocks from different areas have different chemical compositions. That is to say, the results and conclusions from studies in a small region may not fit for the whole region.

Bingsong et al. (2004) found that the lowest layer in siliceous rocks stratum was rich in hydrothermal related elements, which was the evidence of the existence of an upwelling ocean current. In this study, the sample JLK-01 taken from the bottom layer of this siliceous rock stratum also showed high contents on several elements such as P, Cu, and Ni. This result seems to be the same as Yu's result. Cautiously, the abnormal data on one sample may come from many reasons that upwelling ocean current may not be the only explanation.

Some studies have reported that some hydrothermal structures including veins and saddle crystals were founded at the top part of Qigebuluk Formation, which is just laid under the siliceous rock stratum. The hydrothermal

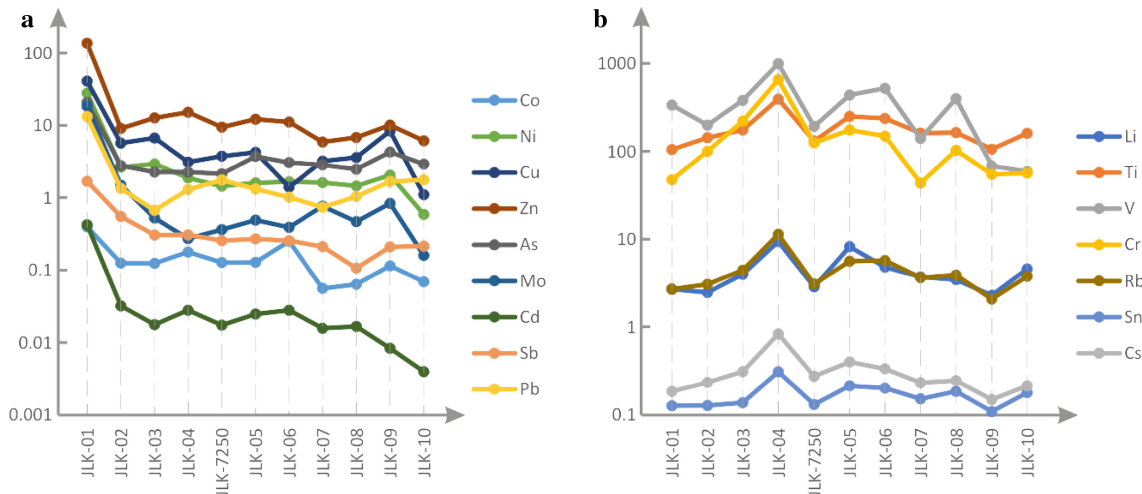


**Fig. 7** Trend of elements content on JLK section, the unite of Y-axis is ppm ( $10^{-6}$ ). From left to right (JLK-01 to JLK-10), the order is from bottom to top

activity, which made these structures also formed these siliceous rocks. However, some studies did not support this opinion. Qian et al's. (2014) study showed that these structures formed at the penecontemporaneous stage or later. Because of the hiatus between Qigebuluk Formation and Yuertus Formation, the formation time of these structures may be much earlier than siliceous rocks' formation.

## 7 Conclusions

At the bottom of Yuertus Formation in Northwestern Tarim Basin, Keping, a siliceous rock stratum appeared. This stratum included layered siliceous rocks and banded siliceous rocks sandwiched in dolomite. After analyzed its major elements and trace elements composition, we draw the following conclusions.

First, all samples have low Ge/Si ratios, and these values are range from 0.15 to 0.37  $\mu\text{mol/mol}$ . These values are much lower than the siliceous rocks formed by hydrothermal activity. The contents of hydrothermal related elements in these samples are much lower than typical hydrothermal formed siliceous rocks. The evidence shows that these siliceous rocks' main siliceous source is seawater instead of hydrothermal fluid.

Second, the samples' Th/U ratios are all lower than 1. Furthermore, the Ce/Ce\* of these samples ranges from 0.88 to 0.99, much higher than normal seawater. This evidence shows that these siliceous rocks were formed in a reducing environment.

Third, these siliceous rocks are rich in Al. The samples' average Al/(Al + Mn + Fe) is higher than 0.8. The average value of Ce/Ce\* of these samples is about 0.95. This value is between the ocean basin type (0.55) and the continent margin (1.34). Considering the evidence from geochemical and sedimentology, the tectonic environment of siliceous rocks in Yuertus Formation is a continental shelf.

Fourth, JLK-01 is rich in Fe, P, As, Cu, and Mo and much higher than other samples. The upwelling ocean current may be the reason.

**Acknowledgements** This study is financially supported by National Key Basic Research Program of China (973 Program, No. 2012CB214801). We also thank Prof. Dong Lin at Peking University for the help in the ICP-OES analyses.

## References

- Adachi M, Yamamoto K, Sugisaki R (1986) Hydrothermal chert and associated siliceous rocks from the northern Pacific their geological significance as indication of ocean ridge activity. *Sed Geol* 47(1–2):125–148
- Bi Z, Qian L, Tao Y (2016) Matrix effect on barium oxide and hydroxide formation during ICP-MS measurement and its implication for Eu correction. *Geol J China Univ* 22(3):467–473 (In Chinese)
- Boström K, Peterson MNA (1969) The origin of aluminum-poor ferromanganese sediments in areas of high heat flow on the East Pacific Rise. *Mar Geol* 7(5):427–447
- Chen Y, Jiang S, Zhou X et al (2010)  $\delta^{30}\text{Si}$ ,  $\delta^{18}\text{O}$  and elements geochemistry on the bedded siliceous rocks and cherts in dolostones from Cambrian strata. *Tatim Basin Geochimica* 2:12 (In Chinese)
- Chunlong C (2001) Some problems in the study of the siliceous rock. *J Mineral Petrol* 21(3):100–104 (In Chinese)
- Cui Y et al (2019) Germanium/silica ratio and rare earth element composition of silica-filling in sheet cracks of the Doushantuo cap carbonates, South China: constraining hydrothermal activity during the Marinoan snowball Earth glaciation. *Precambr Res* 332:105407
- Dehairs F, Chesselet R, Jedwab J (1980) Discrete suspended particles of barite and the barium cycle in the open ocean. *Earth Planet Sci Lett* 49(2):528–550
- Deng S (2017) Detailed sedimentary texture characterizing and fluidic reforming process tracing of Lower Cambrian platform margin in the Tarim basin. *Peking University, Beijing* (In Chinese)
- Dong L, Shen B, Lee CTA et al (2015) Germanium/silicon of the Ediacaran–Cambrian Laobao cherts: implications for the bedded chert formation and paleoenvironment interpretations. *Geochem Geophys Geosyst* 16(3):751–763
- Douville E, Bienvenu P, Charrou JL et al (1999) Yttrium and rare earth elements in fluids from various deep-sea hydrothermal systems. *Geochim Cosmochim Acta* 63(5):627–643
- Froelich PN, Mortlock RA, Shemesh A (1989) Inorganic germanium and silica in the Indian Ocean: biological fractionation during (Ge/Si) opal formation. *Global Biogeochem Cycles* 3(1):79–88
- Froelich PN, Blanc V, Mortlock RA et al (1992) River fluxes of dissolved silica to the ocean were higher during glacials: Ge/Si in diatoms, rivers, and oceans. *Paleoceanogr Paleoclimatol* 7(6):739–767
- German CR, Holliday BP, Elderfield H (1991) Redox cycling of rare earth elements in the suboxic zone of the Black Sea. *Geochim Cosmochim Acta* 55(12):3553–3558
- Guan W, Hualing L, Jing R et al (2013) Characterization of oxide interference for the determination of rare earth elements in geological samples by high resolution ICP-MS. *Rock Mineral Anal* 32(4):561–567 (In Chinese)
- Hamade T, Konhauser KO, Raiswell R et al (2003) Using Ge/Si ratios to decouple iron and silica fluxes in Precambrian banded iron formations. *Geology* 31(1):35–38
- Hesse R (1989) Silica diagenesis: origin of inorganic and replacement cherts. *Earth Sci Rev* 26(1–3):253–284
- Hujin C, Xuelei C, Lianjun F et al (2009) Redox Sensitive Trace Elements as Paleo environments Proxies. *Geological Review* 55(1):91–99 (In Chinese)
- Jia C (1997) Tectonic characteristics and petroleum Tarim basin China. Petroleum Industry Press, Beijing (In Chinese)
- Jewell PW (2000) Bedded barite in the geologic record. Special Publications of SEPM, New York, pp 147–161
- Li YF, Fan TL, Zhang JC et al (2015) Geochemical Changes in the Early Cambrian Interval of the Yangtze Platform, South China: implications for Hydrothermal Influences and Paleocean Redox Conditions. *J Asian Earth Sci* 109:100–123
- Liu J, Zheng M (1993) Geochemistry of hydrothermal sedimentary silicalite. *Acta Geologica Sichuan* 13(2):110–118 (In Chinese)
- McLennan SM (1989) Rare earth elements in sedimentary rocks: influence of provenance and sedimentary processes. *Geochem Mineral Rare Earth Elements Rev Mineral* 21:169–200

- Mortlock RA, Froehlich PN (1987) Continental weathering of germanium: GeSi in the global river discharge. *Geochim Cosmochim Acta* 51(8):2075–2082
- Mortlock RA, Froelich PN, Feely RA et al (1993) Silica and germanium in Pacific Ocean hydrothermal vents and plumes. *Earth Planet Sci Lett* 119(3):365–378
- Murray RW (1994) Chemical criteria to identify the depositional environment of chert: general principles and applications. *Sed Geol* 90(3–4):213–232
- Murray RW, Buchholtz ten Brink MR, Jones DL et al (1990) Rare earth elements as indicators of different marine depositional environments in chert and shale. *Geology* 18(3):268–271
- Murray RW, Buchholtz ten Brink MR, Gerlach DC, Russ GP, Jones DL (1991) Rare earth, major and trace elements in chert from the Franciscan Complex and Monterey Group, California: assessing REE sources to fine grained marine sediments. *Geochimica Cosmochimica Acta* 55:1875–1895
- Qian Y, Du Y, Chen D et al (2014) Study on sequence boundary and sedimentary facies of Qigebulake formation in Xiaoerbulake section, Tarim Basin. *Pet Geol Exp* 36(1):1–8 (**In Chinese**)
- Sun S, Chen J, Liu W et al (2004) Geochemical characteristics of cherts of lower Cambrian in the Tarim Basin and its implication for environment. *Petrol Explor Dev* 31(3):45–48 (**In Chinese**)
- Sun X, Chen J, Zheng J et al (2008) The Characteristics of rare gas isotope composition in siliceous rock from the bottom of the lower Cambrian in the northern Tarim Basin. *Sci China Ser D-Earth Sci* 38(S2):105–109 (**In Chinese**)
- Taylor SR, McLennan SM (1985) The continental crust; its composition and evolution. Blackwell Science Ltd, London, pp 57–72
- Treguer P, Nelson DM, Van Bennekom AJ et al (1995) The silica balance in the world ocean: a reestimate. *Science* 268(5209):375–379
- Yin X, P Lu, Deng X et al (2015) Geochemistry characteristics of Keping uplift Early Cambrian siliceous rocks and its implications. *J Guilin Univ Technol* 35(5):1–6 (**In Chinese**)
- Yu B, Chen J, Li X et al (2004) Rare earth and trace element patterns in bedded-cherts from the bottom of the lower cambrian in the Northern Tarim Basin, Northwest China: implication for depositional environments. *Acta Sedimentol Sin* 22(1):59–66 (**In Chinese**)
- Zhang W, Guan P, Jian X et al (2014) In situ geochemistry of lower paleozoic dolomites in the northwestern Tarim basin: implications for the nature, origin, and evolution of diagenetic fluids. *Geochem Geophys Geosyst* 15(7):2744–2764
- Zhang JP, Fan TL, Algeo TJ (2016) Paleo-marine environments of the early cambrian yangtze platform. *Palaeogeogr Palaeoclimatol Palaeoecol* 443:66–79
- Zhenju D, Congqiang L, Shuzhen Y et al (2000) REE composition and implication of hydrothermal sedimentation of seafloor. *Geol Sci Technol Inf* 19(1):27–30 (**In Chinese**)
- Zhiqin X, Sitian L, Jianxin Z et al (2011) Paleo-Asian and Tethyan tectonic systems with docking the Tarim block. *Acta Petrol Sinica* 27(1):1–22 (**In Chinese**)
- Zhou Y, Liu J, Chen D (2000) Thread and knowledge to fossil seafloor hydrothermal sedimentation of South China. *Bull Mineral Petrol Geochem* 19(2):114–118 (**In Chinese**)